# Design Guidelines for High-Capacity Bevel Gear Systems

**Raymond J. Drago**
**Boeing Helicopter, Philadelphia, PA**

**Abstract:** The design of any gearing system is a difficult, multifaceted process. When the system includes bevel gearing, the process is further complicated by the complex nature of the bevel gears themselves. In most cases, the design is based on an evaluation of the ratio required for the gear set, the overall envelope geometry, and the calculation of bending and contact stresses for the gear set to determine its load capacity. There are, however, a great many other parameters which must be addressed if the resultant gear system is to be truly optimum.

A considerable body of data related to the optimal design of bevel gears has been developed by the aerospace gear design community in general and by the helicopter community in particular. This article provides a summary of just a few design guidelines based on these data in an effort to provide some guidance in the design of bevel gearing so that maximum capacity may be obtained. The following factors, which may not normally be considered in the usual design practice, are presented and discussed in outline form:

- Integrated gear/shaft/bearing systems
- Effects of rim thickness on gear tooth stresses
- Resonant response

**Nomenclature**

D = Harmonic index, integer D = 0, 1, 2...
f = Tooth mesh frequency and harmonics
k = Integer multiplier, k = 1, 2, 3...
n = Number of gear teeth
N = Rotational speed, revolutions per second
Q = Number of mesh points on gear
$W_D$ = Weight of helicopter damping ring, pounds
$W_G$ = Weight of gear rim, pounds
n = Natural frequency, Hertz

### Integrated Gear/Bearing/Shaft Systems

Bevel gears are typically manufactured as blanks and then attached to their shafts by a variety of techniques including keys, bolts, splines, and the like. The existence of these joints increases the weight and complexity of the finished assemblies while reducing their reliability, accuracy, and effective load capacity. In spite of these limitations, the two-piece shaft and gear assembly remains the most common configuration because it is the easiest system to design and manufacture. In addition, bearing journals are provided for assembly of bearing races, resulting in a multipart gear/bearing shaft assembly with many potential faying surfaces.

In applications in which weight and reliability are critical considerations, these joints and faying surfaces have been the subject of considerable research. The primary operational problem with these joints is fretting. Under the combined conditions of high stress and a fretted surface, a crack can initiate at this joint and, if undetected, can progress to failure. This problem is significant for the typical helicopter application; thus, much effort has been devoted to coatings, platings, lubricants, and similar devices aimed at reducing the long-term effects of fretting and the ensuing corrosion. The obvious final solution to the problem is, of course, the elimination of the joints and faying surfaces altogether. This can be accomplished either by welding or by designing integral gear/bearing/shaft configurations. The former technique has worked well in many applications, but introduces potential new problems associated with the weld itself. The optimum solution is, therefore, integral design. Because of the complex geometry of bevel gears and the offset generat-

ing motions of the cutting and grinding machines, this is easier said than done, especially in the case of complex shafts with projections at both ends of the gear.

The original impetus behind the growth of this technology was the development of the CH-47D helicopter. A decision was made to eliminate all bolted bevel gear joints, either through integral design or welding. Integral design was selected because of lower developmental costs and greater inherent reliability.

The first step in the design of complex, integral-shaft spiral bevel gears is the definition of the path of the cutter with respect to the gear blank. We have developed a computer program which uses manufacturing machine settings to produce plots of the path of various points on the cutting and grinding tools, as Fig. 1 shows.

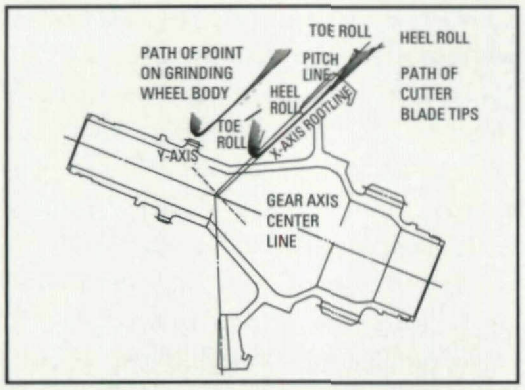


**Fig. 1 - CH-47D forward sun/bevel gear with grinding wheel tip and body point plots.**

Graphic layouts and model checks are used to ensure that a proper cutter and shaft design can be obtained in order to achieve an integral gear design. Machine and cutter modifications have been developed to achieve these results.[1]

Based upon these developments, all of the CH-47D spiral bevel gears were designed to eliminate all bolted or splined joints. A typical comparison of the CH-47C and CH-47D forward transmission sun/bevel gears is shown in Fig. 2. The concept of integral design was extended beyond the elimination of the bevel gear bolted joint to total integration. For this gear this included the integration of an accessory spur gear and a journal for bearings. The final design of the CH-47D sun/bevel gear incorporated three bearing journals and three gears (two spur and one bevel) into a single integral shaft/gear design.

Fig. 3 also shows the integral bevel gears for the aft and engine transmissions. The engine transmission bevel gear required a significant design change in the center portion in order to

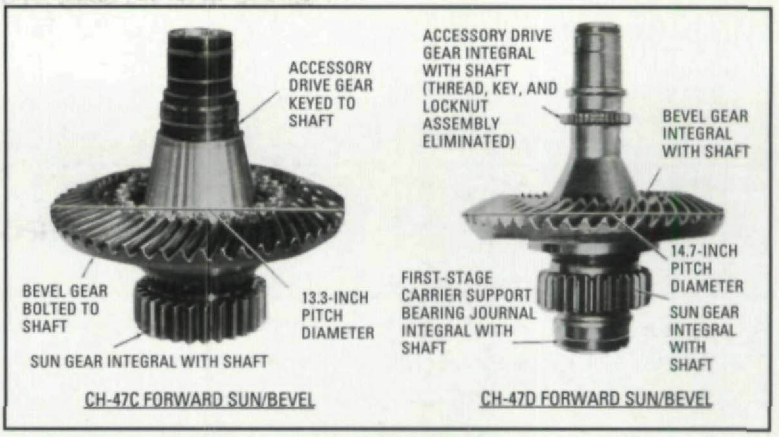


**Fig. 2 - Comparison of CH-47C and CH-47D gears.**

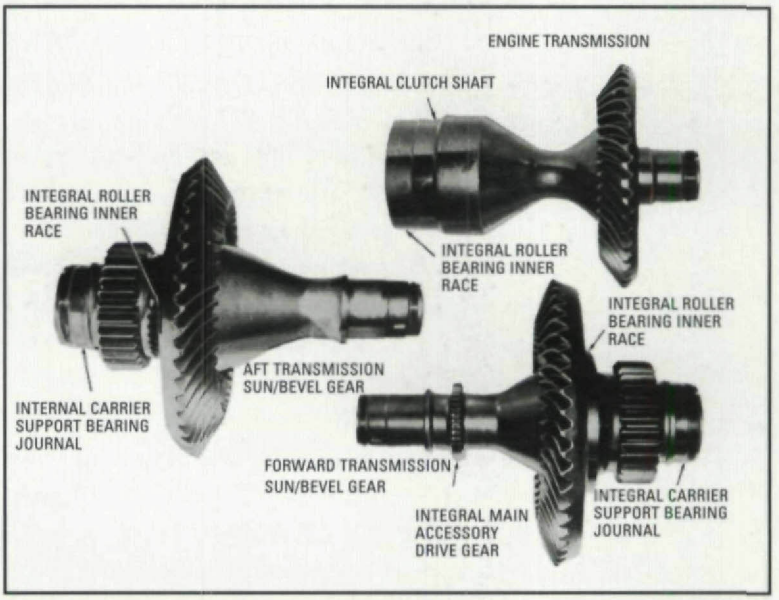


**Fig. 3 - Representative example of a integral spiral bevel gears for the CH-47D helicopter.**

eliminate cutter interference.

Furthermore, the power transmitted per pound of gear has been increased, as shown in Table 1, by at least 10% and as much as 20% for the growth power level of the CH-47D bevel gears (10,000-hp system) as compared to the CH-47C gears (6,000-hp system). The philosophy of integral design has been taken several steps further in the CH-47D transmissions, permitting a more compact (relative to power transmitted) and more reliable drive system than that of the CH-47C. All of these improvements have been made without significantly increasing the gear tooth stress levels over those of the CH-47C.

The projected production acquisition cost of the integral CH-47D gears is virtually the same as that for the conventional bolted shaft assembly, while the life-cycle cost will be significantly lower because of reduced rejections at overhaul for joint-related problems. The rejection rate is quite high for such problems; thus, eliminating the joint will greatly lessen rejects. This conclu-

**Raymond J. Drago**
*is Associate Technical Fellow, Dynamic Systems Technology, at Boeing Helicopters. He is the author of numerous books and papers on gearing subjects.*

**Table 1**
Relative Weights of CH-47C Bolted Flange and CH-47-D Integral Bevel Gears

| Transmission | CH-47C (6,000-hp system) (hp/lb) | CH-47D (10,000-hp system) (hp/lb) | Percent Improvement |
|---|---|---|---|
| Forward | 89 | 102 | 15 |
| Aft | 96 | 105 | 10 |
| Mix | 123 | 147 | 20 |
| Engine | 175 | 209 | 20 |

sion must be tempered somewhat, since with the integral gears a non-repairable defect on the gear or shaft will result in the entire component's being scrapped, whereas with separate parts, this is not the case. This is a small consideration within the context of the overall system and is far overshadowed by the improvements in weight, reliability, and life-cycle cost.

## Effects of Rim Thickness on Gear Tooth Stresses

Many investigators have indicated that the accuracy and applicability of currently available equations for predicting gear tooth bending stress are limited in some applications. Testing and actual field experience have verified the fact that gears which are constructed in such a way that the rim supporting the gear teeth is less than rigid have tooth root stresses that differ substantially from those predicted by conventional theory.

In order to overcome the shortcomings of the existing analytical tools, several researchers have addressed the problem in a variety of ways. Some have proposed new approaches based on variations of simple beam theory, while others have used finite-element methods (FEM). In addition to these analytical efforts, many photoelastic and strain survey investigations have been conducted.

Unfortunately, the vast majority of the research (both analytical and experimental) has concentrated on the gear teeth themselves without regard to the blank configuration. This research has been demonstrated to be inadequate for lightweight, thin-rimmed gears. In order to better understand this phenomenon, a series of investigations was undertaken with a simple segment model. The results of this testing clearly indicated that the root stresses become much more significant as the gear rim thickness is reduced.

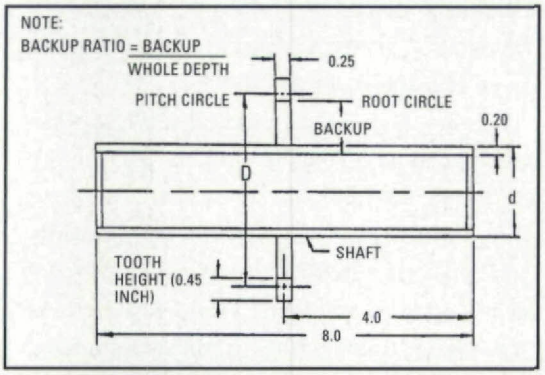


**Fig. 4 - Photoelastic test specimen configuration.**

In order to accurately evaluate the effect of rim thickness, three different pitch diameters combined with five rim thicknesses were evaluated, as summarized in Table 2, in an extensive series of photoelastic tests.[2-3] In order that the date from each test specimen could be directly compared, the gear tooth configuration was the same on all specimens, as shown in Table 3.

The gear blank construction was also designed to be representative of an actual blank, as shown in Fig. 4. The pitch diameter (D) and shaft bore diameter (d) were the parameters varied during the test. Radial support was provided for the model at each end of the shaft, and one end was clamped to provide torsional restraint.

In contrast to these test specimens, virtually all photoelastic gear testing done before this investigation was conducted with large tooth-segment specimens. For example, in their landmark work on stress concentration factors, Dolan and Broghamer used two-pitch, 14.5° and 20° pressure angle tooth segments. (Fig. 5).

The gear tooth form for each specimen was defined by a computer program developed as a preprocessor for a gear FEM analysis system.[4] This program provided accurate point-by-point coordinate data for both the profile and fillet areas. These data were transferred to a Gerber 4400 plotting system on magnetic tape. This computer-based system then scaled up the data by a factor of 10 and provided sequential tooth plots on Mylar.® The system enabled the plot accuracy to be controlled within a few thousandths of an inch. These plots were subsequently used to manufacture the actual specimens.

A line-master copy milling machine was used to cut the gear teeth on all specimens. The 10-times-size gear tooth plots were placed on the copy mill tracer table and converted optically back into digital coordinate data. The machine then reduced the digital data to actual size and used the signal thus produced to guide an end-milling cutter which cut the actual tooth profile. The speed of the cutter was kept high and the feed rate low, so that the resultant parts had good accuracy and finish; the accuracy of the finished

parts was about AGMA Quality Class Q 11.

Two-dimensional models were fabricated from annealed polycarbonate plastic for the 8:1 through 2:1 specimens. These gears were then bonded to aluminum-filled epoxy shafts which were modulus-matched to the plastic blank material (solid aluminum shafts were, however, used for the 4- and 8-inch pitch diameter, 7.5:1 and 3.8:1 backup gears, respectively, to prevent excessive lateral shaft deflection).

Three-dimensional models were required for all the 0.45:1 specimens because the rim thickness was only slightly greater than the shaft wall thickness. The 3-D specimens were cast from an epoxy-based resin system employed phthalic anhydride and amine hardeners; the castings were then machined to the appropriate dimensions. In order to facilitate cutting the teeth on the copy mill, the 3-D shafts were parted near the gear tooth area and rebonded after the teeth were cut. Fig. 6 shows a variety of the specimens used.

The 2-D model assembly - model, load arm, and model restraint - was placed in the optical path of a transmission polariscope, which permits the analysis of the isochromatics (lines of constant color) through the use of circularly polarized light. The shaft was restrained radially at both ends and torsionally at one end, while the load was applied to the central tooth of the five-tooth cluster. Load was applied at three separate locations along the tooth profile: low point of single-tooth contact (LPSTC), pitch line (PL), and high point of single-tooth contact (HPSTC). An isochromatic color photograph (35mm slide ) was obtained at each load location for subsequent analysis and documentation. The model was then modified to the next configuration by removing the gear from the shaft, enlarging the gear inside diameter, and bonding to a shaft of larger diameter (2:1 backup ratio).

The 3-D photoelastic models were loaded as shown in the test schematic in Fig. 7. All three positions, LPSTC, PL, and HPSTC, were loaded simultaneously to conserve time because of the "stress-freezing" procedure, which involves a detailed heating and cooling cycle. Subsequent to the "stress-freezing" procedure, the model was sliced by machining off the ends of the shaft so that a constant-thickness, 2-D model through the gear tooth section remained. The slice was placed in the polariscope and analyzed exactly as the 2-D specimens were.

**Table 2**
Photoelastic Test Specimen Configuration Gear

| Dia. D (in.) | Shaft Dia. d (in.) | Backup Ratio | Dash No. | Model Type |
|---|---|---|---|---|
| 16 | 8.70 | 8:1 | 1 | 2D |
| 16 | 14.00 | 2:1 | 2 | 2D |
| 16 | 15.40 | 0.56:1 | 3 | 3D |
| 8 | 0.75 | 7.5:1 | 4 | 2D |
| 8 | 6.10 | 2:1 | 5 | 2D |
| 8 | 7.40 | 0.56:1 | 6 | 3D |
| 4 | 0.75 | 3.8:1 | 7 | 2D |
| 4 | 2.10 | 2:1 | 8 | 2D |
| 4 | 3.40 | 0.56:1 | 9 | 3D |

**Table 3**
Test Gear Tooth Geometry

| | |
|---|---|
| Diametral Pitch | 5.000 |
| Pressure Angle | 25.000 |
| Addendum | 0.200 |
| Dedendum | 0.245 |
| Fillet Radius | 0.062 |
| Tooth Thickness | 0.310 |
| Tooth Form | Involute |
| Root Configuration | Circular fillet with no undercut |

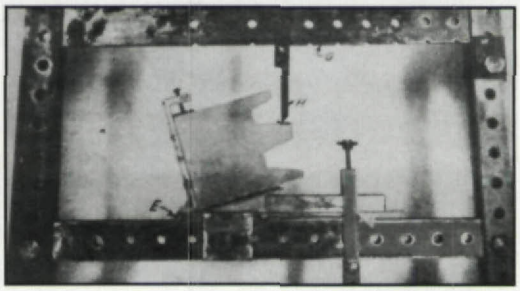

**Fig. 5 - Dolan and Broghamer test setup.**

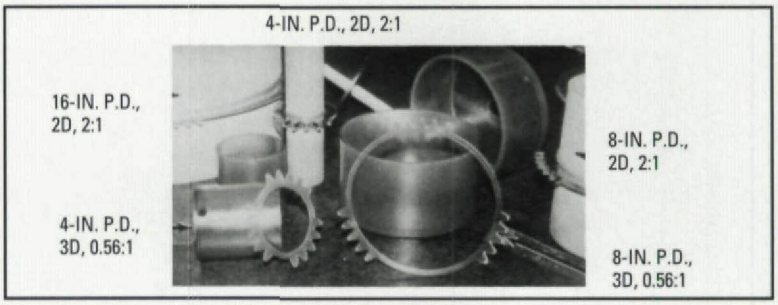


**Fig. 6 - Comparison of 2-D and 3-D test specimens.**

The photoelastic stress analysis was performed by the color-matching technique, whereby colors of known magnitude are matched to those of the projected image. The ability to discern partial fringe orders is typically ± 0.1 fringe, assuming an initial fringe order of approximately 0.7 or more. Therefore, the accuracy of this technique is directly related to the magnitude of the observed fringes. Throughout this test program, the majority of analyzed fringes were 2 or more, which resulted in an accuracy of ± 5% or better.

The data obtained from the experiments were

reduced and converted into stresses. The magnitudes of the stresses of and by themselves are of little consequence, since we are primarily seeking trends. Furthermore, since the models were plastic, the loads and the resultant stresses were quite low relative to those which one would expect on a metal gear of the same size. Despite these facts, it is always interesting to compare experimental data to some known points. We have already indicated that for gears with relatively large rim thicknesses, the conventional equations predict the maximum fillet tension stress with reasonable accuracy. In order to verify this observation, measured fillet tension stresses for the test specimens with the largest backup ratios were plotted as functions of load position. This plot, Fig. 8, shows that the tension stress at the highest point of single-tooth contact (HPSTC) is quite close to the predicted by the conventional equations. The actual deviation varies from about + 8% to + 13%, which is reasonably good correlation.

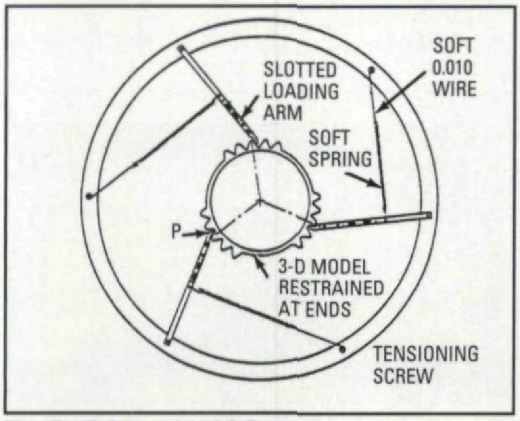


**Fig. 7 - Schematic of 3-D test setup.**

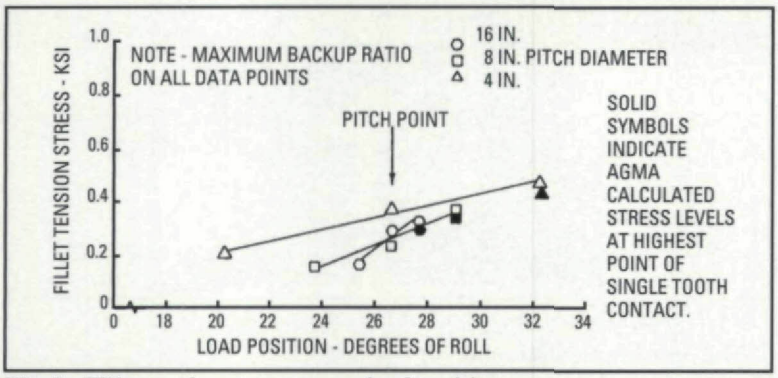


**Fig. 8 - Fillet tension stress versus load position.**

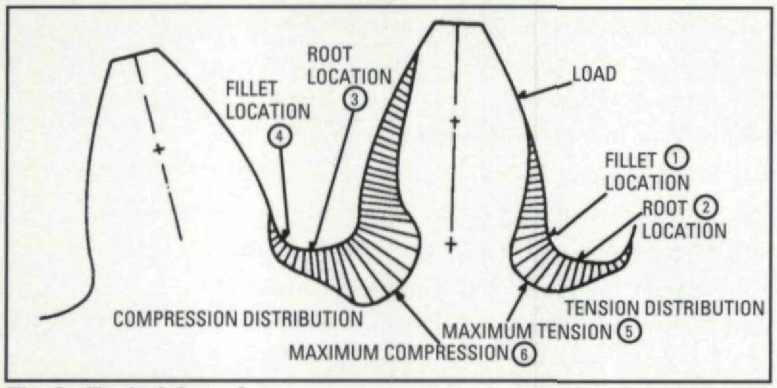


**Fig. 9 - Typical data plot.**

The stress index calculated with the conventional AGMA equations is based on the maximum tension stress. In fact, however, it is the maximum alternating stress which determines the fatigue load capacity of a gear tooth. With this in mind, most of our ensuing discussion will center on alternating stress levels. Before discussing the actual data, it would be wise to establish some conventions for naming the stress of interest. All of the raw data were reduced to produce plots of tensile and compressive stress as shown in Fig. 9 (which is the fringe data plot for the 4" pitch diameter, 2:1 backup specimen, loaded at HPSTC) for each combination of pitch diameter and backup ratio. The points identified as fillet locations correspond approximately to the conventional AGMA critical bending section. When we speak of fillet stresses in the ensuing discussion, they have been measured at this location. Similarly, when we speak of root stresses, they have been measured at the root location shown in Fig. 9. This point corresponds to the location of the maximum alternating stress in the root. Generally, it is quite close to the centerline of the space, usually on the tension side.

Clearly, for unidirectional loading, the maximum alternating stress does not necessarily occur at the same location as either maximum tension or maximum compression. For bidirectional loading (e.g., idler gear), the maximum alternating stress is usually the result of the combination of maximum tension and maximum compression.

Although we measured stresses with the load applied at several points along the tooth profile, the maximum alternating stresses occurred when the load was applied at the highest point of single-tooth contact. Our discussion will thus be limited to this load case for all models.

One of the first results which became apparent was that, while the trend was apparent, we could not define a firm diameter effect. Our attempts to define a rim thickness effect were much more successful. A large amount of data resulted from this testing, and the interested reader may consult Ref. 3 for more detailed information.

In our analysis of these data, many parameters were plotted and evaluated. Perhaps the most significant are the fillet and root alternating stress and the alternating stress for fully reversed loading shown in Figs. 10-12.

Although many subtle effects may also be noted, the main trend shown in these plots is quite apparent: the stress increases dramatically as the rim thickness-to-whole depth ratio drops below 2:1. The conventional AGMA equations show no such effect. It is also interesting to note that the measured stresses remain reasonably constant as the backup ratio increases above 2:1.

Another parameter which is of interest is the alternating stress that occurs when the gear is subjected to a fully reversed load, as is the case for an idler gear. As expected, the alternating stress level is substantially higher than for either the root or fillet locations when subjected to unidirectional loading. For a given allowable stress level, the load capacity is thus lower when a gear is used as an idler. This fact is by no means a startling revelation. Most designers incorporate a reduction factor when calculating idler gear load capacities. AGMA standards recommend that the allowable stress be reduced to 70% of its unidirectional value for bidirectional loading. Actually the allowable stress does not change; rather, the magnitude of the alternating stress changes. Thus, applying the correction to the allowable index stress in accordance with the AGMA standards is a convenience rather than a factor. In order to define the actual reduction to be expected, we have plotted the ratio of root alternating stress to the fully reversed alternating stress in Fig. 13.

Based on these data, it appears that the 70% suggested by the AGMA standards is a bit optimistic for small diameters, but is certainly reasonable overall.

We have clearly established the fact that the measured stresses are quite different from the calculated stresses. The calculated stresses are, however, stress indexes rather than exact stress levels. The difference between calculated and measured would then be much less significant if a constant relationship existed between the two. It should be obvious that this is not the case, since we have already demonstrated that the measured stresses vary substantially with backup ratio, while the calculated stresses do not.

Plots of test data clearly indicate that a constant relationship does not exist, at least backup ratios below 2, between the actual stress levels and the conventionally calculated index stresses. These data may, however, be used to develop a rim thickness factor, $K_B$, which can be used to improve the accuracy of the conventional equations. Fig. 14 shows this factor with data from both the photoelastic test program and an investigation which used the FEM analysis to be discussed in the next section superimposed on the curves. The development and use of this factor are covered in more detail in Ref. 5, and the reader should consult this paper before applying $K_B$ in design.

While these data have been developed with spur gear models, the basic trends apply to all types of gears. Great care must be exercised when applying these results to bevel gears with complex blanks, particularly those with T-shaped sections. The hard point over

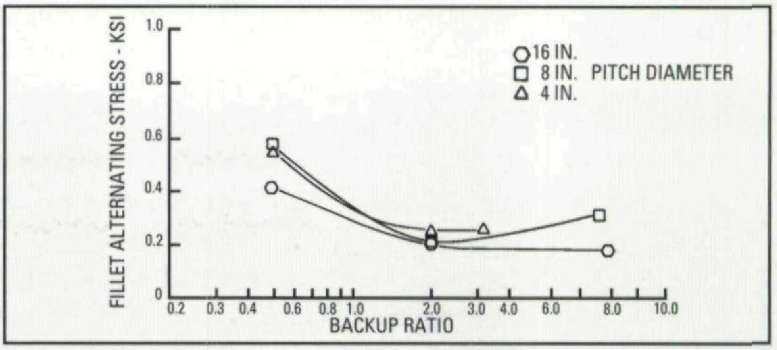


**Fig. 10 - Effect of backup ratio on fillet alternating stress.**

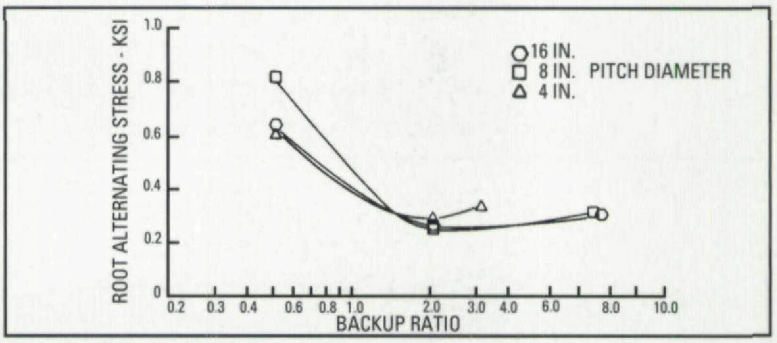


**Fig. 11 - Effect of backup ratio on root alternating stress.**

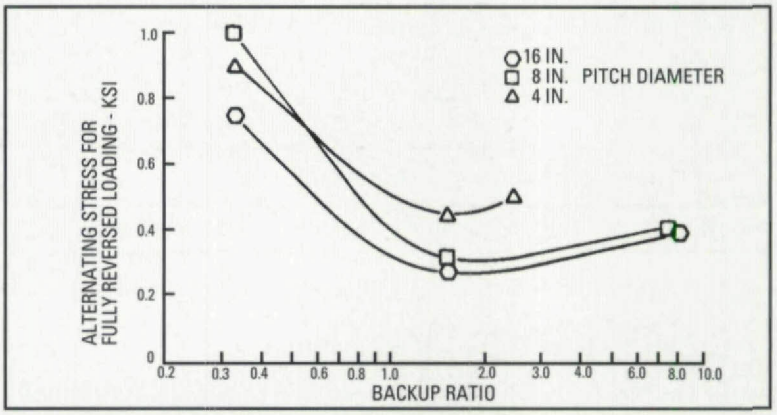


**Fig. 12 - Alternating stress for fully reversed loading.**

the center section can act as a concentration point for root stresses, further aggravating a bad situation.

### Resonant Response

Gear resonance is one of the most insidious and destructive of all gear failure modes. It generally occurs quite suddenly and with catastrophic results. Since a gear often fails by the separation of large fragments from the blank, the damage is usually extensive, especially when high rotational speeds are involved.

The prevention of this type of failure is relatively simple once resonance has been identified as the causative factor. Either of two approaches may be taken: The gear can be redesigned so that its natural frequencies do not coincide with any operational excitation condition; or the blank can be damped so that even if excited at its natural frequency, the response of the gear is small enough to preclude failure.

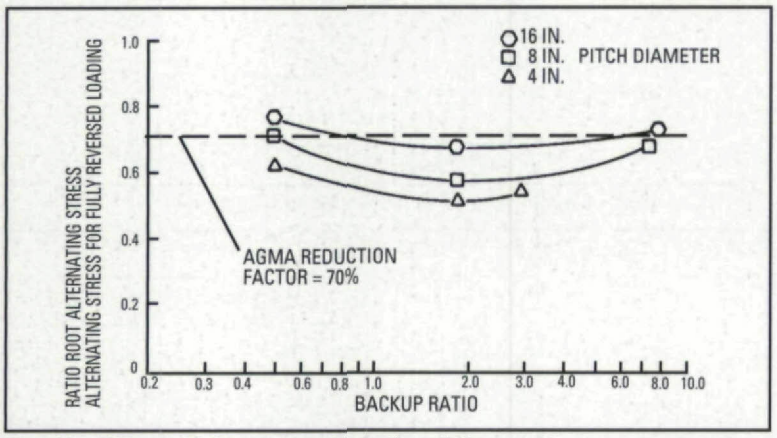


**Fig. 13 - Effect of fully reversed bending (idler gear) on root stresses.**

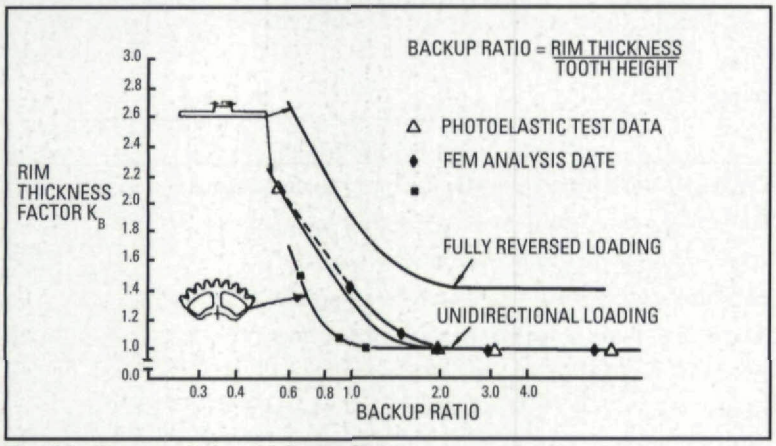


**Fig. 14 - Proposed rim thickness factor.**

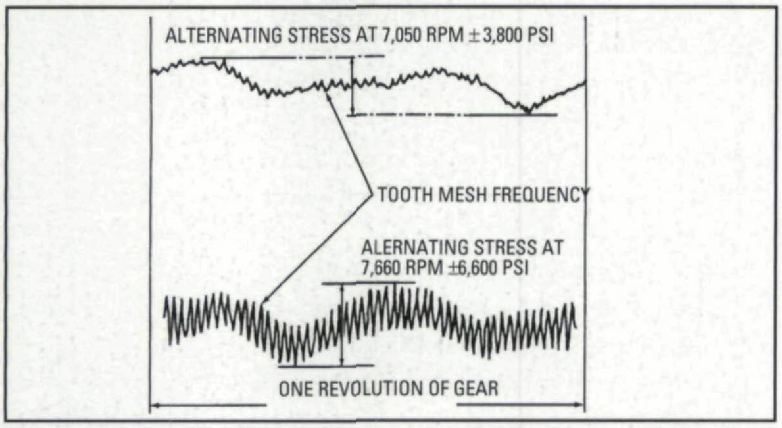


**Fig. 15 - Increase in alternating stress resulting from speed change to excite resonant response.**

Resonance phenomena in gears, while not widely treated in the literature, can be of considerable consequence in the design of high-speed, lightweight gearing. Should the blank be excited at a frequency sufficiently close to one of its resonant frequencies, deflections and, hence, stresses can increase to levels where failure can occur within a relatively short time. Fig. 15 shows the increase in stress resulting from operation near a resonant frequency. Stress plots were obtained from telemetered strain-gage readings during dynamic transmission tests. Strain gages were located on the flange of a spiral bevel gear. It is interesting to note that although the torque remained constant, a change in shaft speed of less than 9% resulted in an increase in stress level of over 73%. In this example, a further increase in speed of about the same magnitude would cause the stress level to fall again to the 3,800 psi range. The narrow speed band sensitivity is characteristic of gear resonance problems.

The origin of resonant failure is at or near the outermost part of the blank in the gear tooth root, where the combined tooth-bending and blank resonance stresses are maximum. The crack progresses through the blank as shown in Fig. 16 and returns to the gear outer diameter, thus removing a wedge-shaped fragment from the blank. Gears which suffer this failure mode are usually, but not always, operating at high rotational speed; thus the high-energy fragment causes considerable damage, as Fig. 16 demonstrates. Because of the catastrophic nature of the

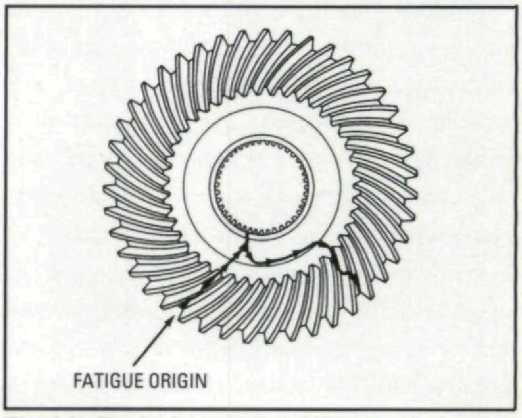


**Fig. 16 - Typical resonance failuer.**

failures associated with this phenomenon, it is possible that it will not be recognized as the causal agent, and a general beefing-up of all parts involved is undertaken as a fix for the problem. In many cases, this will solve the problem, since the resonant frequencies will also be altered; however, the resulting design is usually heavier and more costly than necessary. Had the resonant problem been recognized and dealt with, the final configuration would have been more cost- and weight-effective.

*Mode Shapes* - When a body is excited at its natural frequency, the body will assume an oscillating deformed shape called a mode shape. For a body of revolution these mode shapes can be generally classified by the number of nodal diameters (diameters exhibiting zero displacement) occurring during the vibration deformation cycle. The number of nodal diameters contained in a mode shape is referred to as the harmonic index of the mode. Classification of modes by their characteristic harmonic index is helpful, not only as an aid in visualizing the mode shape, but also in the determination of excitation frequencies. In theory, a body of revolution is capable of an infinite number of mode shapes for each value of harmonic index. These mode shapes are all unique and occur at unique characteristic natural frequencies. The mode shapes consist of various combinations of circumferential or ring nodes, i.e., circumferential rings of zero displacement. Fig. 17A is a sketch of the deformed mode shape of a thin-walled cylinder (solid line) superimposed on the undeformed shape of the cylinder. This particular mode has a harmonic index of 2, as evidenced by the number of nodal diameters. Note the circumferential ring node occurring at section B-B. Fig. 17B shows the cylinder again responding in a harmonic index = 2 mode, but at a higher frequency and with ring nodes at sections E-E and G-G.

*Speed/Frequency (Campbell) Diagrams* - It is important to note that the mode shapes shown in Fig. 17 represent the displacements at an instant in time; at 1/2 cycle or 1/2 $\omega_n$ seconds later, the displacements of the structure will be the negative (with respect to the undeformed shape) of the displacements shown. With this in mind, it can be seen that for a stationary (nonrotating) circular disk or cylinder, a rotating, steady (non-oscillating) force will induce constructive reinforcement of the displacement waves at a rotation speed of

$$N = \pm \omega_n / D \qquad (1)$$

By a simple change of reference system it can be seen that this is also the case for a rotating circular structure subjected to a force stationary in space. This relationship is valid for values of harmonic index D = 1, 2, 3... For the case of D = 0, no nodal diameters (purely axisymmetrical mode shape), this criterion does not apply, since a nonoscillating rotating force will not excite this type of displacement mode shape. The excitation forces for gear tooth meshing forces are not steady, but oscillate with respect to a reference system fixed to the rotating gear. The frequency of oscillation of the mesh forces and their harmonics is

$$f = knN \qquad (2)$$

for k = 1, 2, 3... Hence, the criterion to produce constructive reinforcement of a displacement mode shape by a rotating, oscillatory, exciting force is

$$\omega_n = knN \pm DN = (kn \pm D)N \qquad (3)$$

A convenient method of displaying the rela-

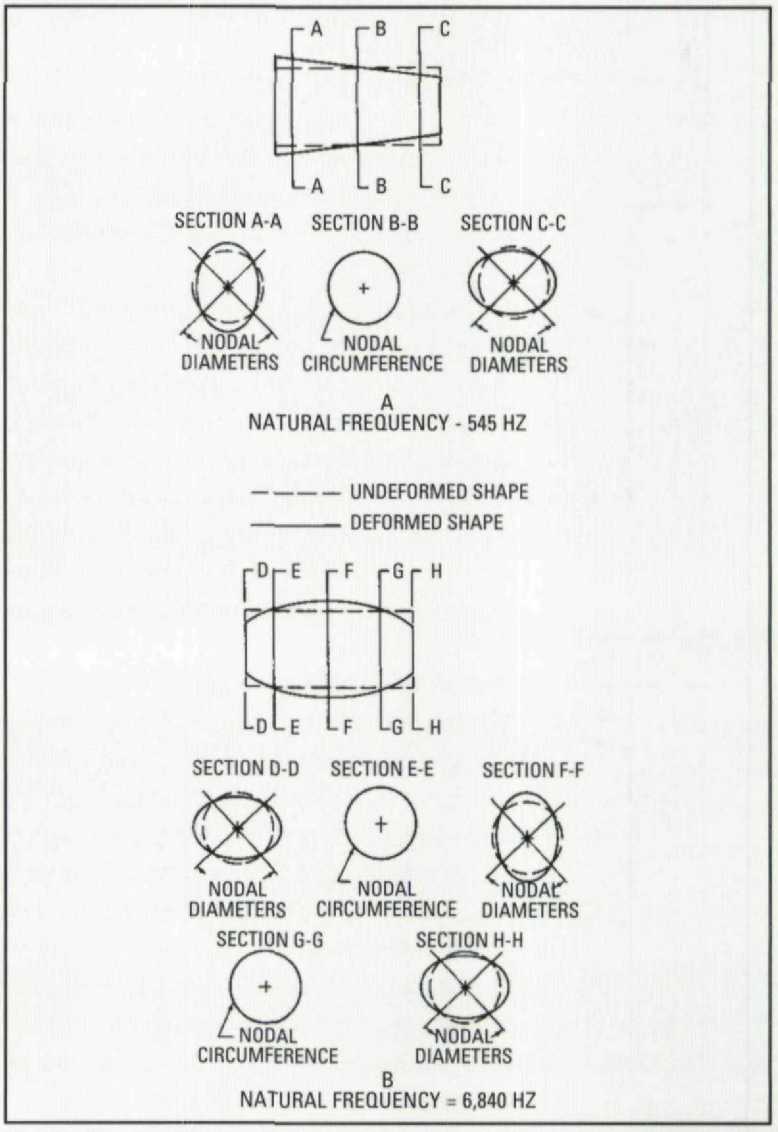


**Fig. 17 - Sketch of two mode shapes of harmonic index = 2 for hollow cylinder.**

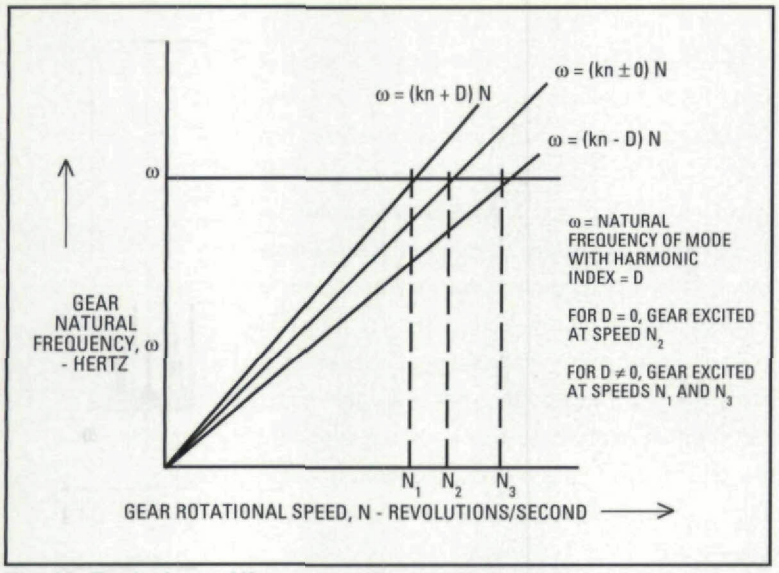


**Fig. 18- Typical speed/frequency (Campbell) diagram.**

tionship between gear natural frequencies and transmission system excitations is with a frequency-versus-speed diagram. Excited frequencies are plotted on the vertical axis and rotational speed is plotted on the horizontal axis as shown in Fig. 18. Such charts are frequently referred to as Campbell diagrams.

Natural frequencies from bench test or analysis are plotted as horizontal lines. The lines $\omega_n = (kn \pm D)N$ are then plotted for the values of D corresponding to the mode shapes of the natural frequencies under consideration. The points where the horizontal $\omega_n$ lines intersect the $\omega_n = (kn \pm D)N$ lines indicate the speeds at which the gear resonance will be excited. Should these speeds occur within the operating speed range, a potential gear vibration problem will exist. Resonant conditions can also be excited by harmonics of the tooth mesh frequency; therefore, $n = (kn \pm D)N$ should be plotted for several of the lowest values of k. In addition, other potential sources of excitation must be considered. One which is of particular importance in the design of epicyclic gear systems is the planet passage frequency. Note that for modes with a harmonic index of 1 or greater, resonance conditions are excited at two speeds for each tooth mesh harmonic. The case of a harmonic index = 0 mode is excited only at the basic tooth mesh frequency and its harmonics. In all cases the frequencies at which the gear vibrates are its natural frequencies with respect to a reference frame fixed to the rotating gear. It should be noted that the apparent stiffness of the rotating gear can be slightly altered by centrifugal effects, thereby causing n to be a function of rotational speed. If this function can be determined either by test or analysis, the foregoing is still applicable. In this case the $\omega_n$ horizontal lines would become $\omega_n = f(N)$ curves, and the intersection points would be determined as described previously. For gear sizes and speeds typically encountered in vehicle power gearing, these centrifugal effects have been found to be negligible.

*Evaluation of Resonance Behavior* - The problem of evaluating the resonance behavior of a specific gear may be approached in many ways, however, these methods can be broadly classed as either experimental or analytical. Experimental techniques provide very accurate data regarding response frequencies and mode shapes; however, actual hardware (or at least prototype gears) is required. This limits the correction of any problem areas identified to either redesign or add-ons. The use of analytical techniques, on the other hand, allows these problems to be addressed and corrected in the design stage. The basic data sought by either method are the response (resonant) frequencies, the mode shapes, and the level of response; i.e., the stresses induced by operating at a resonant frequency. Both methods can provide the first two pieces of the puzzle, frequency and mode shape; however, the level of response can usually be obtained only thorough the use of sophisticated strain-gage instrumentation during an actual operational transmission run. Some progress is being made in the analytical definition of response level. Although it would seem that analytical techniques are preferable in all cases, advantages and disadvantages to both methods will become clear as we proceed thorough the next two sections. One of the biggest unknown factors is the amount of damping that occurs because of bolted joints, supports, and the like.

Experimental Methods - There are many methods for experimentally defining the resonant frequencies and mode shapes of gears. The specific method which should be used in any particular case is a function of component size, mass, and the dollars available for test.

In order to evaluate the response of a part, an excitation source and some means of detecting the response and defining the mode shape must be provided.

The testing is generally conducted as follows: The gear is mounted in such a way that it is isolated from its surroundings (elastomeric pads, cords, etc.) and excited with a variable-frequency

source. A sweep through the frequency range of interest is performed while the gear response is monitored. Frequencies which produce substantial responses are noted. After the frequency sweep is completed, the gear is again excited at each of the noted frequencies while the gear is searched or probed to define the mode shape.

The determination of frequencies to be searched can be enhanced by performing a simple bang test if frequencies have been calculated previously by some analytical method, or should a frequency spectrum analyzer be available. Fig. 19 shows a typical spectrum-analyzer oscillograph from gear bang testing. Note the number of frequencies which display high relative response; these frequencies represent the excitation frequencies near which gear resonant problems may occur. Note also the large number of resonant frequencies. A bang test consists simply of hitting the gear once and evaluating the resulting response with the aid of a spectrum analyzer. A gear thus excited will ring down at all its natural frequencies; with a spectrum analyzer, these frequencies can be separated and identified.

This experimental technique actually determines the free-vibration characteristics of the gear; however, the natural frequency of free vibration has been an excellent indicator of the installed and operating resonant frequencies of the gear and shaft. Fig. 20 is a Campbell diagram showing the free-vibration resonant frequencies of an integral spiral bevel gear and shaft, as determined from air siren testing versus shaft speed. Also plotted on this diagram are the frequencies at which increased response was noted for the component installed and operating under design loadings. These operating data were obtained from telemetered strain-gage readings recorded during a transmission dynamic strain survey. Note that the forced-response frequencies of the operating gear and shaft agree closely with the free-vibration natural frequencies determined in siren tests.

The four main variables to be addressed in an experimental investigation of the resonant response of a gear (or any other part) are the method of excitation, the method of detecting when a resonant condition has been encountered, the method of identifying the mode shape of a particular response, and the stress level associated with a particular response. With the

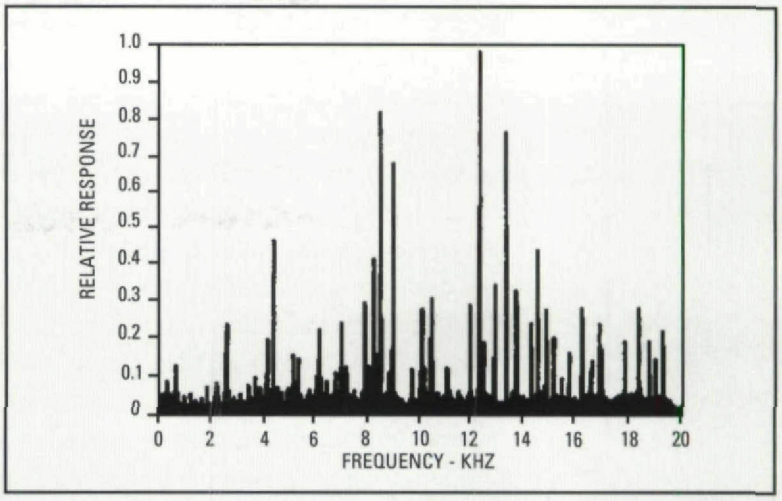


**Fig. 19 - Typical plot of relative response amplitude versus frequency from gear bang test.**

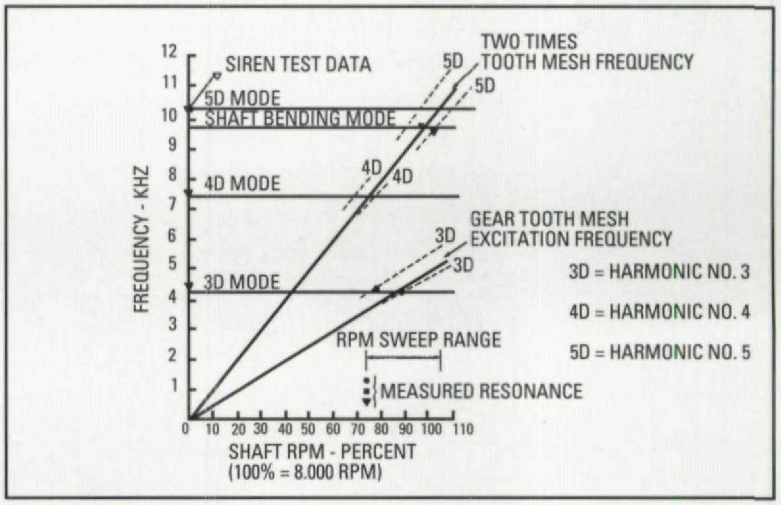


**Fig. 20 - Campbell diagram showing siren test and operating resonant frequency response.**

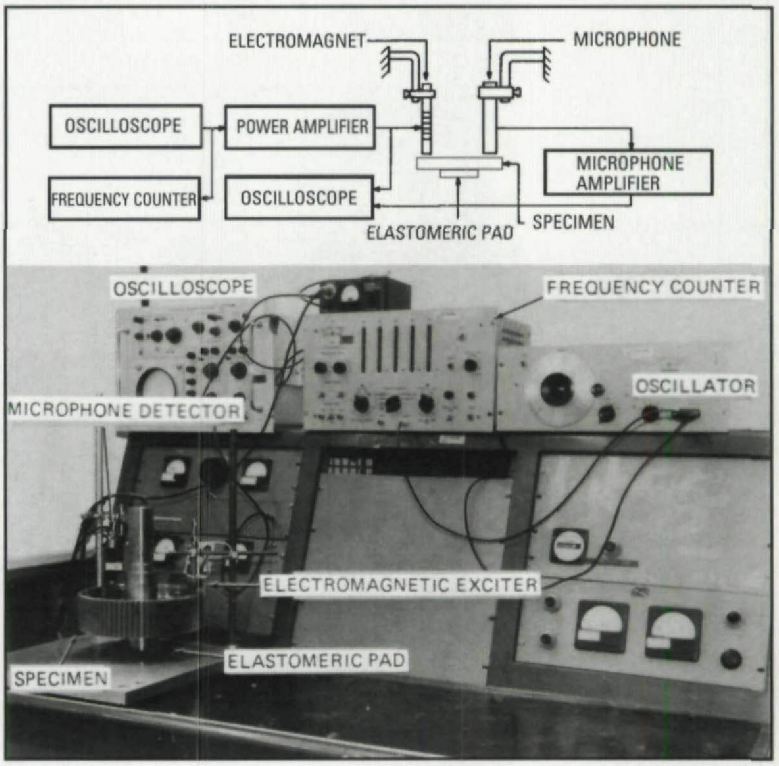


**Fig. 21 - Electromagnetic excitation with detection by microphone and oscilloscope.**

exception of the stress level, each parameter may be addressed separately since, in theory at least, any excitation method can be used with any combination of detection and identification techniques. However, considerations of experimental setup and procedure will limit the combinations which are practical. Complete descriptions of the various techniques can be found in Ref. 6. An excitation source, such as the electromagnetic setup shown in Fig. 21 or the air siren shown in Fig. 22, is the first piece of equipment required. A means of detecting the existence of a resonant frequency, such as the microphone shown in Fig. 21 or the accelerometer shown in Fig. 22, is also required. Finally, the mode shape itself must be defined through the use of sand or glitter patterns (Fig. 23), holography, or by hand-probing with a microaccelerometer (Fig. 24).

If a strong excitation source is used, hand-probing (Fig. 24) with a microaccelerometer can identify nodes and antinodes and, thus, mode shapes. This technique does require some operator skill and practice on simple shapes. It can be very useful in the evaluation of complex modes on complex gears.

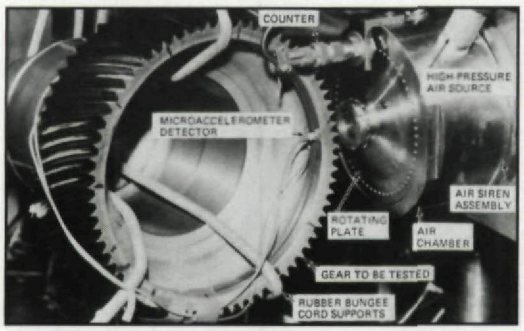


**Fig. 22 - Air siren excitation source.**

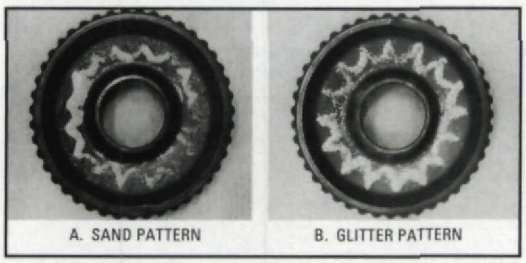


**Fig. 23 - Mode shape detection on a flat spiral bevel gear (17,939 Hertz).**

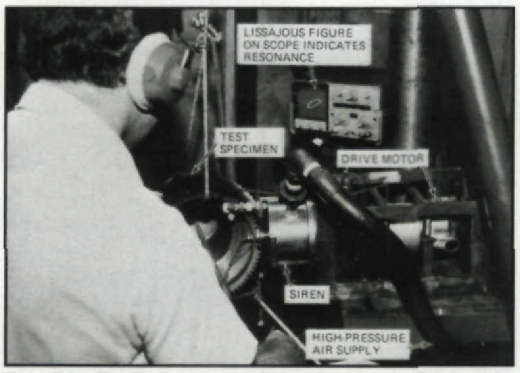


**Fig. 24 - Technician probing manually for mode shapes.**

Analytical Methods - The high costs associated with the redesign of complex gears to improve their dynamic characteristics after initial prototype fabrication and testing make necessary accurate analytical techniques with which to predict resonance. This would allow the design engineer to predict the dynamic characteristics of a particular gear design while it is still on the drawing board, thus enabling any changes to be incorporated before fabrication and test.

Because of geometrical complexity and the generality of configuration, the finite-element method (FEM) was chosen as the most suitable analytical technique. Recent experience using several general-purpose FEM computer programs and modeling techniques indicates that excellent correlation with experimental data from prototype resonant testing is possible. The most efficient of these techniques has been an axisymmetrical modeling approach. This method assumes the gear to be symmetrical about its rotational centerline and, hence, requires that only a single cross section be modeled.

The model definition required for sufficient-ly accurate results (that is, within about 5-10% overall) is quite coarse relative to that required for tooth or blank stress analysis. The teeth themselves, for example, are not modeled as separate entities; rather, only their mass is simulated. This is done by increasing the root diameter to the midtooth diameter and then modeling the gear teeth as a solid ring of this thickness; in most cases this modeling system yields excellent results. For many lower modes (which are the most important anyway) the accuracy is far better than that at higher modes; in most cases the error is less than 5%.

Some of the difference between bench and dynamic rig test results may be because of centrifugal stiffening of the blank at normal operating speed. However, when we consider the good overall correlations obtained at low to moderate speeds, this effect can be considered negligible. This may not be the case for very high-speed, large-diameter gears.

Most programs include the ability to produce a plot of each mode shape, which can be quite helpful in determining which areas of the gear require modification to obtain the desired dynamic characteristics. One such plot is shown in

Fig. 25. Each mode shape has an associated harmonic index. This index represents the integer number of nodal diameters characteristic of the nodal displacement shape of the gear. Fig. 25 also shows an axial view of the deformation of the integral spiral bevel gear shaft, indicating that the harmonic index of this mode is 3. The analytically predicted and measured resonant frequencies are also compared. The correlation in this particular case is exceptionally good; in general, the predicted values for the lower frequencies do not differ more than 5% from the measured siren test frequencies.

*Modifying Resonance Behavior*- Once the resonant frequencies have been determined, it must be ascertained whether the frequencies lie in the operating excitation range. If resonances do occur in the operating frequency range, the design engineer is faced with a decision: He may either modify the design (change mass and/or stiffness of the gear), or he may provide some form of damping to decrease the response of the gear near the resonant frequency.

Both approaches have inherent advantages and disadvantages. A careful evaluation of the alternatives is required in order to decide which method is applicable to any given situation.

Detuning - Modifying the geometry of the gear in an effort to change its mass and/or stiffness characteristics is frequently referred to as detuning. The ideal approach is to design all gears so that their natural frequencies are far from any potential excitation sources, especially gear mesh and its multiples.

Although this approach is not practical in all cases, it can be eminently successful, particularly if the blank is relatively simple and the Campbell diagram is uncluttered; such a case is shown in Fig. 26. The gear mesh frequency at overspeed (3,682 Hertz) is quite close to a natural frequency (3,764 Hertz). Adding material as shown increased this natural frequency beyond the overspeed excitation frequency. In this instance the next lower frequency did not increase enough to bring it into proximity with either the idle or 100%-speed excitation sources. In cases such as this, plots of the mode shape are an invaluable aid in determining where and how the gear must be modified.

Since each problem is unique, no hard-and-fast guidelines can be given on the methods to be used in accomplishing such modification, but it is generally best to make changes which increase stiffness and, thus, raise the natural frequencies, rather than to add mass alone, such as adding lumps to the gear bore. This method has been shown to be the most weight-effective for lightweight gearing.

This discussion is aimed at small perturbations of a basically fixed design. If an analysis is performed early enough in the design cycle, it may be possible to make a major change which will effectively improve the situation.

Damping - If detuning is not practical or not successful, damping is a viable alternative. Damping causes the amplitude of and, hence, stress response to the excitation forces to be reduced in the installed and operating forced - response environment. If the proper amount and type of damping are applied at the appropriate places on the gear blank, this approach is almost always successful. There are many ways in which damping can be introduced into the blank. In addition, the construction of the gear itself may contribute to its damping characteristics. If it is manufactured as a separate part and is bolted, keyed, or splined to its shaft, the joint will provide a small amount of damping through the rubbing action (Coulomb damping) which is inevitable at such joints. Unfortunately, this motion, which is beneficial in a damping sense, can be very detrimental over the long term, since it may give rise to fretting. Fretted joints can be the source of cracks in either gear or shaft which lead ultimately to structural failure. An integral shaft and gear design eliminates both the damping and

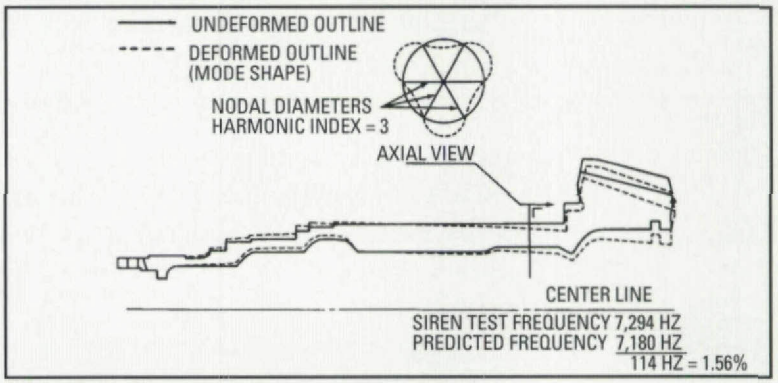


**Fig. 25 - Predicted gear resonant frequencies.**

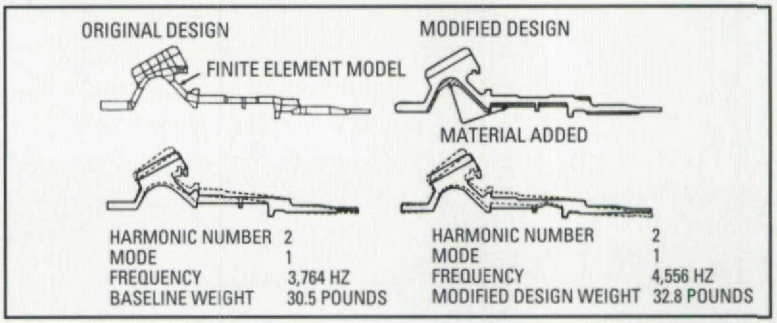


**Fig. 26 - Comparison of original and modified spiral bevel gear designs; modification improved resonant frequency characteristics.**

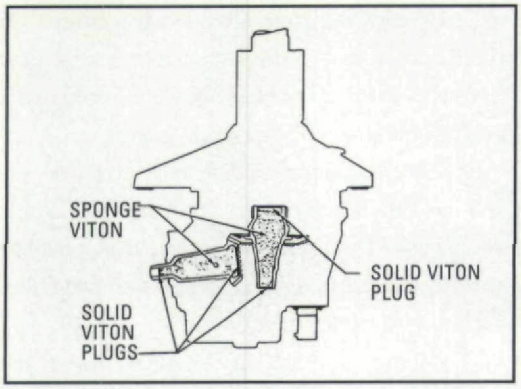


**Fig. 27 - Hollow gear shafts filled with elastomer and plugged.**

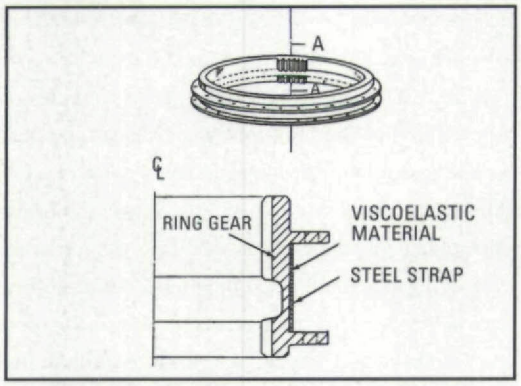


**Fig. 28 - Thin elastomeric coating on gear web *with steel constraint.***

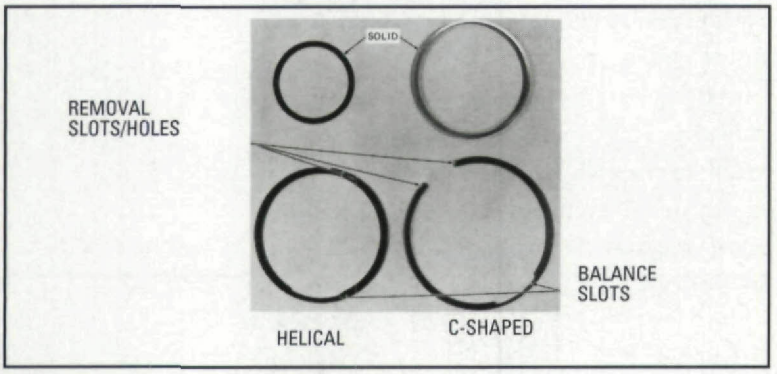


**Fig. 29 - Types of damping rings.**

fretting conditions and is preferable, since fretting can be a major problem, and there are other less severe and more effective methods of applying damping. Two of the simplest methods are coatings and rings.

Coatings - *Coatings can be applied to nonfunc*tional surfaces of the gear blank to reduce the vibration level. Both hard and soft coatings have been used with varying degrees of success. Soft coatings, such as bonded layers of an elastomer, have been used in a number of applications. Because they are exposed to the hot oil environment, they generally must be either trapped as shown in Fig. 27 or constrained as shown in Fig. 28. The effectiveness of either method depends upon maintaining the bond between the elastomer and the gear blank. Other methods of coating, such as plasma-spray coating or electrochemically plating relatively heavy metals like molybdenum or copper compounds on the appropriate surfaces, are more permanent and less likely to separate from the gear.

Any of these methods will work, particularly if the response is not overly energetic, and if the gear design incorporates large, flat web areas; however, our testing has shown that while the noise level is reduced in many cases, the damping provided is not sufficient to reduce the vibratory stresses to acceptable levels.[8]

Rings - Damping rings are a much more effective method of providing damping. Solid, C-shaped, and helical rings (Fig. 29) have been used successfully. Solid rings are inserted into an internal groove machined under the gear rim by heating the gear and cooling the ring. Helical rings, which are actually modified common retaining rings, are turned into a similar groove in the gear rim. Both dissipate energy through a mechanism which is believed to be largely Coulomb friction at the sides and, especially, the bottom of the groove. The helical rings provide considerably more damping (about 2.5 times more, according to Ref. 8) than solid rings, and both provide an order-of-magnitude more damping than most coatings, though they are generally not as effective in reducing noise as some coatings appear to be. The solid rings have less retention surface (limited by the amount of gear expansion and ring contraction at installation); thus, they are more likely to fall out of their grooves and cease their damping function because of wear than are helical rings, which typically have relatively deep retention grooves. In addition, the force exerted on the groove by a solid ring does not increase appreciably with rpm because of centrifugal force (CF). Since helical rings are not closed loops, they tend to unwind with increasing CF and exert greater force and, thus, greater damping on the ring groove. In a similar manner, the damping effectiveness of helical or C-shaped rings is not affected by wear, since CF will keep opening the ring so that contact is maintained with the groove. After solid rings wear, CF only contributes to increased ring stress and does not maintain contact pressure with the groove; thus, damping effectiveness may decrease substantially. In order to yield maximum effectiveness, the proper amount of ring weight must be provided. The results of extensive dynamic strain survey testing have been analyzed in an effort to determine the ring weight required in the

general case. Based on this information, the following empirical relation between ring weight and gear weight has been developed:[9]

$$W_D = 0.06 W_G 0.75Q \qquad (4)$$

Equation 4 has been shown to work well for lightweight aircraft-type gears in the size range of 6" to 33" pitch diameter and at pitch line velocities up to approximately 28,000 fpm.

The importance of the proper choice of ring weight and placement can be seen in Fig. 30. The final stress level has been reduced by 50%, even though the transmitted torque increased by more than 80%.

One of the most significant problems associated with damping rings is the wear that occurs both on the ring and its groove. Although the groove wear alone is almost never severe enough to cause the gear to fail, slivers which can cause indications on chip detectors, indicating screens, and other debris monitors can be generated. In addition, the ring wears excessively when its cross section is reduced, and the possibility of its failure arises. These problems can be reduced by hardening the groove and using multiple-wrap rings. The wear appears to be caused more by the ring being forced to rotate in its groove by the gear-load-induced deflections under the mesh point than by its vibration in the groove because of its response to gear natural frequencies. It seems likely that the wear problem could be reduced by decreasing these deflections.

The addition of damping rings or coatings does not change the natural frequencies of the gear to any measurable extent; this has been verified by electromagnetic and air siren testing as well as full-scale transmission testing.

Changing Excitation Frequency - Our discussion thus far has been limited to modifications of the response of a gear to a given excitation source. It is also possible in some cases to change the excitation frequency. This can be done in several ways. The easiest but usually the least practical method would be simply to alter the system speed so that it does not coincide with any of the natural gear frequencies. Relatively large changes in excitation frequency can also be made by changing the diametral pitch (module) of the gear set to increase or decrease the number of teeth, thus changing the mesh frequency without changing shaft speed. Any change in pitch should be carefully evaluated in order to insure that the bending-fatigue capacity of the gear set is not compromised. Several design techniques have been proposed to employ gearing

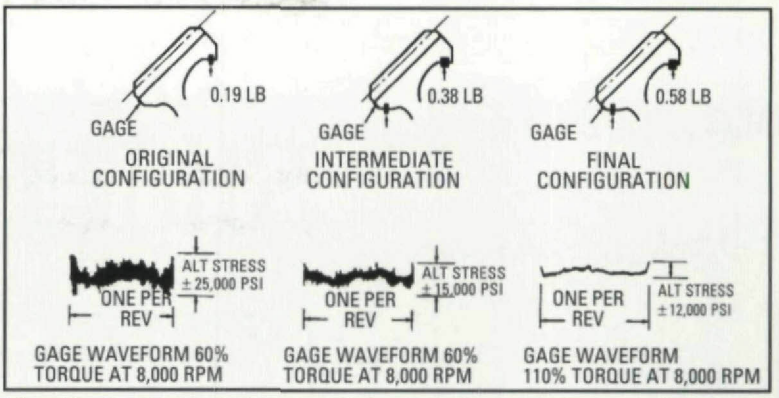


**Fig. 30 - Reduction of transmission bevel gear response through increased damping.**

with either more or fewer teeth than would ordinarily be used on a given sized gear.

Other alternatives, which would require redesign, are to alter the number of planets in an epicyclic system or to change the relative ratios used in each stage of a multipass system.

## Conclusions

Three areas of significant concern to the designers of spiral bevel gearing have been identified and discussed. Each area is outside the normal design procedures for such gears, but can be very important in the overall success of specific designs.

General design guidelines have been presented and references for further and more detailed studies have been provided. ■


**References:**

1. DRAGO, RAYMOND J. "On the Design and Manufacture of Integral Spiral Bevel Gears for the CH-47D Helicopter," Aerospace Gearing Committee Meeting, AGMA, March, 1978.
2. DRAGO, R.J. and PIZZIGATI, G.A. "Some Progress in the Accurate Evaluation of Tooth Root and Fillet Stresses in Lightweight, Thin-Rimmed Gears." Paper P229.21, AGMA, October, 1980.
3. DRAGO, R.J. and LUTTHANS, R.V. "An Experimental Investigation of the Combined Effects of Rim Thickness and Pitch Diameter on Spur Gear Tooth Root and Fillet Stresses." Paper P229.22, Fall Technical Meeting, AGMA, October, 1981.
4. DRAGO, R.J. "On the Automatic Generation of FEM Models for Complex Gears - A Work-in-Progress Report." Aerospace Gearing Committee Meeting, AGMA, February, 1982.
5. DRAGO, R.J. "An Improvement in the Conventional Analysis of Gear Tooth Bending Fatigue." Paper P229.24, Fall Technical Meeting, AGMA, October, 1982.
6. DRAGO, R.J. and BROWN F.W. "The Analytical and Experimental Evaluation of Resonant Response in High-Speed, Lightweight, Highly Loaded Gearing." Paper 80-C2/DET-22, Century 2 International Power Transmission and Gear Conference, ASME, August, 1980.
7. SCIARRA, J.J. et al. "Helicopter Transmission Vibrations and Noise Reduction Program, USARTL TR 78-2A." Applied Technology Laboratory, U.S. Army Research and Technology Laboratories (AVSCOM), Fort Eustis, VA, March, 1978.
8. MCINTIRE, W.L. "How to Reduce Gear Vibration Failure." Aerospace Gearing Committee Meeting, AGMA, February, 1964.
9. ALBRECHT, C. "Developments in Gear Analysis and Test Techniques for Helicopter Drive Systems." Paper 79-DE-15, Design Engineering Conference and Show, ASME, May, 1979.



*From* Gear Design Manufacturing, Design & Inspection Manual